A ChipSat Swarm for Mars Atmospheric Characterization

Thomas Timmons *, Gilles Bailet †, James Beeley ‡ and Colin McInnes §
James Watt School of Engineering, University of Glasgow, Scotland, UK. G12 8QQ

A mission scenario is proposed where a large number of centimeter-scale femto-spacecraft are dispersed from a CubeSat piggy-back payload on a future Mars mission. This swarm would deliver real-time massively parallel sensing throughout entry, descent, and landing (EDL) with in-orbit measurements, atmospheric characterization during descent, and even surface science upon landing. Since few entry profiles exist at present for the *in situ* atmospheric modeling of Mars, a ChipSat swarm offers a promising tool for cost-effective atmospheric characterization that could lower risks for ongoing Mars exploration programs.

Nomenclature

γ = flight path angle, °

λ = latitude, °

μ = mean molecular weight of air, g/mol

ρ = density, kg/m^3

ϕ = longitude, °

A = cross-sectional area, m

a = acceleration relative to the atmosphere, m/s^2

C_d = drag coefficient

g = acceleration due to gravity, m/s^2

h = altitude, km

h_s = constant density scale height, km

i = inclination, °

m = mass, kg

p = atmospheric pressure, Pa

q = heat flux, kW/m^2

R_0 = universal gas constant, $J/K.mol$

*PhD Candidate, Space and Exploration Technology Group, t.timmons.1@research.gla.ac.uk
†Research Associate, Space and Exploration Technology Group
‡Research Associate, Space and Exploration Technology Group
§James Watt Chair, Professor of Engineering Science, Space and Exploration Technology Group

r_n = nose radius, cm

T = atmospheric temperature, K

v = velocity, km/s

I. Introduction

The twin Mars Cube One (MarCO) CubeSats launched with the Insight mission [1] highlighted the potential that low-cost and high-risk piggy-back payload opportunities have for technology demonstrations on interplanetary missions. In this case, the success of the two 6U CubeSats in providing a communications relay with the Insight Lander and Earth during EDL may lead to a new design approach to similar missions in the future. Although using the characteristically small CubeSat standard, as candidate piggy-back payloads on interplanetary missions, the relatively large size and mass of these platforms renders them unrealistic options for applications such as multi-point sensing, atmospheric characterization [2], distributed field and particle measurements or surface science [3], where there exists significant spatial and temporal variability. For these purposes, we consider that a swarm of even smaller spacecraft could be deployed from a CubeSat to fulfill such applications by enabling data to be gathered simultaneously across a range of spatial length scales. Previous studies have considered using such devices as atmospheric entry probes [2].

Due to the ongoing trend of miniaturization of technology, for several years now it has been feasible to develop functional spacecraft equipped with an inertial measurement unit (IMU), an attitude determination and control system (ADCS) and wireless RF communications, all mounted on a printed circuit board (PCB) with dimensions of a few square centimeters. Dispersing large numbers of these devices from a CubeSat carrier opens up a wide range of potential applications and future mission scenarios. This concept was pioneered by the KickSat project [4], which deployed over a hundred PCB-based satellites, coined ChipSats [5], from a 3U CubeSat.

ChipSat swarms can enable the collection of large-scale, simultaneous and distributed measurements over a large volume of space to provide future improvements to surveying planetary atmospheres, space weather monitoring, magnetosphere characterization, gravity field mapping and distributed sparse aperture interferometry [6–9]. In this mission scenario, we consider that in-orbit science measurements, atmospheric characterization during EDL and surface science upon landing are all possible with such a piggy-back payload. The low ballistic coefficient of ChipSats means that, depending on the entry trajectory, they need only be equipped with a thin thermal protection system (TPS) to survive the thermal loads encountered during atmospheric entry, with the possibility that a small percentage of the swarm may survive surface impact [2, 10, 11]. The ChipSats could be packed inside the CubeSat with a flexible TPS that deploys after ejection using shape-memory alloy (SMA) struts, as shown in Fig. 1. Consequently, the swarm can characterize the atmosphere of Mars during descent and possibly even conduct surface science upon landing by forming a static ad-hoc wireless sensor network (WSN) during the remaining battery lifetime.

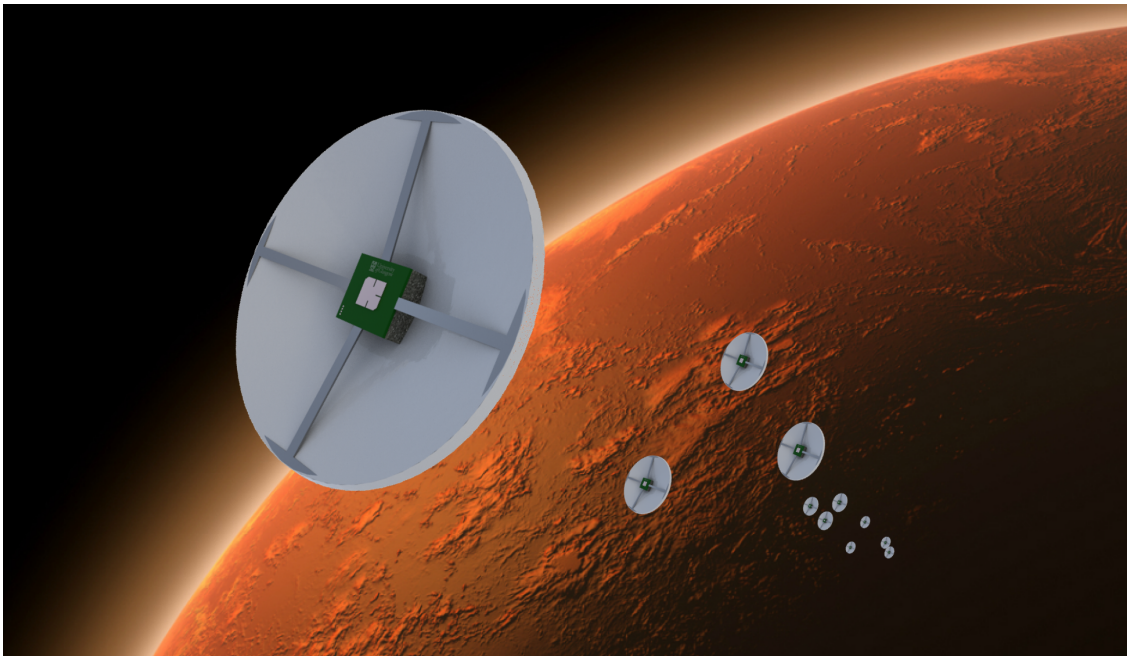

Fig. 1 Concept for a ChipSat Swarm descending into the Martian atmosphere

There are extended functional benefits to using a ChipSat swarm. A high level of overall swarm robustness against failure and individual ChipSat redundancy can deliver robust swarm operations with practically no functionally essential swarm members. The swarm's operations can be made modular and dis-aggregated; different ChipSats can be equipped with different instrumentation and tasked with different roles, and failed units can simply be retired without impacting the overall mission objective. All these attributes increase the probability of mission success and enhance the utility of a ChipSat swarm [12].

At present, few Mars entry profiles are available for atmospheric data reconstruction from *in situ* measurements [13], so a swarm of ChipSats would substantially increase the number of data sets available. A ChipSat swarm presents the opportunity for multiple, near-simultaneous atmospheric entries. Were deployments from the CubeSat carrier to occur for each season on Mars, a more comprehensive understanding of the dynamics of the Martian atmosphere could be achieved. Multiple swarm entry profiles would greatly add to the few *in situ* atmospheric profiles currently available [14], especially for uncertainties in the upper atmosphere and seasonal variations. The configuration proposed in this paper is analogous to real-world Monte-Carlo trajectory propagation and so is an exciting tool for atmospheric characterization at low-cost/high-reward to lower risks for ongoing Mars exploration programs.

The paper is organised as follows. Section II presents the proposed mission scenario. Section III details the swarm entry trajectory modeling, ChipSat thermal properties, atmospheric characterization and relative positioning. Section IV details the ChipSat as a scientific platform, the thermal protection system for Mars EDL, and mass, power and link budgets for the mission scenario.

II. Mission Scenario

In the proposed mission scenario, a swarm of ChipSats is contained within a 12U CubeSat carrier that is a piggy-back payload on a future Mars mission, comparable in terms of size and mass with the MarCO flight opportunity. The CubeSat carrier can deploy the ChipSats either simultaneously or sequentially in sub-groups to deliver real-time, massively parallel sensing. This deployment sequence would be tuned to ensure there is a low risk of collisions between the ChipSats. An 8U volume of the CubeSat carrier would be used to store at least 64 ChipSats while 4U would be reserved for the other CubeSat subsystems. As was demonstrated by MarCO [1], the CubeSat carrier can also provide a data relay between the swarm and Earth, or between the swarm and another satellite in orbit around Mars, such as the Mars Reconnaissance Orbiter. In descent, the ChipSats transmit IMU data and sensor measurements in their wake to the CubeSat carrier using an S-band patch antenna situated on the top of the ChipSat PCB.

The CubeSat would be detached after the last trajectory correction maneuver of the flagship carrier spacecraft. The CubeSat will then deploy the swarm on a trajectory that intersects the Martian atmosphere. ChipSats could be deployed with a Δv in the order of 10 cm/s using a spring-loaded mechanism. Then, the CubeSat will use its own propulsion module consisting of cold gas thrusters to adjust its trajectory to avoid entry and remain above the swarm in order to relay their data. This type of delivery method, involving ejection from a CubeSat that avoids atmospheric entry to provide the data relay with Earth, was explored in [15].

For trajectory modeling and assessment of atmospheric characterization capabilities, similar entry conditions to the previously flown Mars Exploration Rovers have been used, with uncertainties extracted from [16]. During atmospheric entry, each ChipSat will perform attitude rate and acceleration measurements using an IMU comprising micro-electro-mechanical systems (MEMS) gyroscopes and accelerometers to reconstruct their trajectories. Prior to deployment, ChipSats could be connected to power and data lines within the CubeSat, so that their IMUs could be calibrated on-board the CubeSat with a series of slews to register angular and translational accelerations. IMU thermal drift calibration would be performed prior to the flight to account for temperature dependent errors [17]. Additional pressure and other MEMS sensors are envisaged to be implemented on different ChipSats.

The ChipSat swarm would be ejected with a known impulse from the CubeSat and begin to disperse as it translates towards the entry interface point with the Martian atmosphere. Using the radio link to network between the swarm and the deployer it would be possible to gather ranging data that is used by the CubeSat to determine the relative motion and dispersion of the swarm. This is discussed in Section III.D. Throughout atmospheric descent, it would also be possible for the CubeSat to occasionally collect ChipSat velocity data from Doppler shift measurements of the received frequencies as compared to the known transmitted frequencies. This would complement IMU-only trajectory reconstruction.

Upon landing, surviving swarm members could form a static ad-hoc WSN with relative positioning between ChipSats enabled by the RF communication link. This could enable Martian surface science if ChipSats are equipped with

additional sensors, such as mass spectrometers. Regions of the Martian surface that are infeasible to explore with rovers due to the risk involved and difficulty of access, such as the Valles Marineris canyons, are made available as candidates for in-situ analysis of surface composition [18].

III. Entry Trajectories & Atmospheric Characterization

Using on-board accelerometers, each ChipSat will measure their deceleration throughout the descent which will then be post-processed and used to reconstruct their trajectories directly to retrieve position and velocity time history estimates. As no mass loss (ablation) is expected during the entry phase, accelerometers errors that would otherwise arise due to this are considered negligible for the reconstruction. The swarm would disperse after ejection to cover a range of entry conditions.

A. Trajectory Modeling

Trajectory analysis is performed using a three-degree-of-freedom simulation code [17]. An exponential Mars atmosphere model is assumed, with density decreasing exponentially with altitude such that:

$$\rho = \rho_0 \exp\left(\frac{-h}{h_s}\right) \tag{1}$$

where $\rho_0 = 0.02$ kg/m^3 is the atmospheric density at zero altitude and $h_s = 11.1$ km is the (assumed) constant density scale height [19]. We model a direct entry configuration for the swarm dispersed over a range of entry conditions using a sensitivity analysis consisting of 32805 possible EDL trajectories from an evenly spread range of parameter variations. The nominal atmospheric reference entry conditions used are shown in Table 1.

Considering small variations around the nominal entry conditions expected for the swarm (in altitude (h), velocity (v), latitude (λ), longitude (ϕ), inclination (i), entry flight path angle (γ), drag coefficient (C_d) and atmospheric density (ρ)), we can simulate the range of entry trajectories that the swarm may experience, accounting both for the variation in deployment parameters as well as atmospheric uncertainties. The ChipSat mass and reference area are modeled as 65 g and 0.02 m^2. The uncertainty ranges are taken from [16].

In the simulation the ChipSats are assumed to have a nominal drag coefficient $C_d = 1.6$ afforded by the aerodynamically stable thermal shell. Lift is not modeled as ChipSats could be actively spun up at the point of ejection from the CubeSat to help rigidify the structure and negate any unintended lift that could arise. Figure 2 displays 32805 EDL trajectory results from the sensitivity analysis when modeled with the uniform variations shown in Table 1.

The nominal reference trajectory is shown in red, with all other trajectories in black. As expected, the entry profiles and landing dispersion of the swarm is substantially impacted by even small variations and uncertainties in the initial entry conditions. These entry trajectories indicate that a swarm dispersed over a series of possible entry parameters

Table 1 Entry Parameters

Entry Parameter	Nominal Value	Uncertainty Range
h, km	130	± 5.1
v, km/s	5.8	± 0.003
γ, °	-15.2	± 0.06
λ, °	0	± 0.12
ϕ, °	0	± 0.03
i, °	0	± 0.06
C_d	1.6	± 10%
ρ_0, kg/m^3	1.7×10^{-7}	± 10%

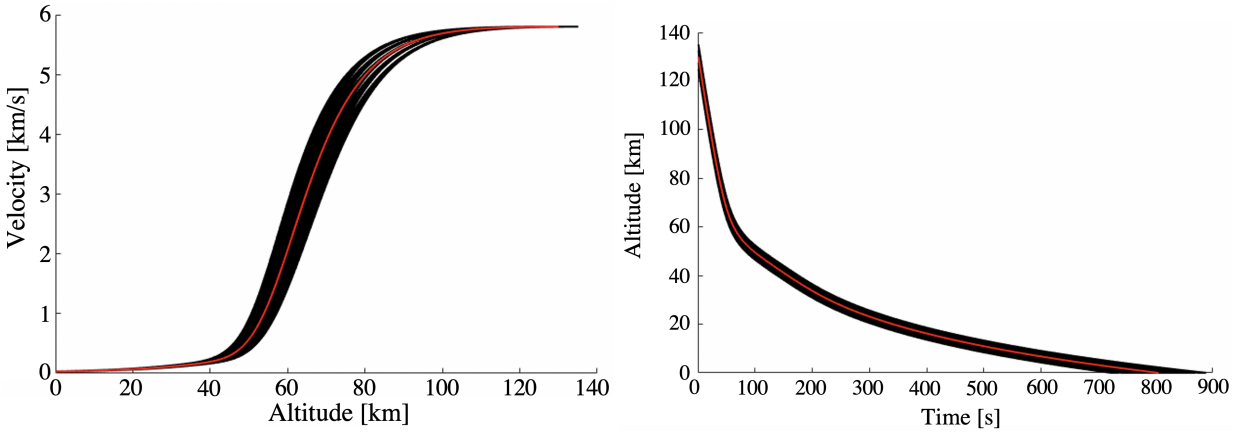

(a) Velocity vs. altitude **(b) Altitude vs. time**

Fig. 2 32805 EDL trajectories from sensitivity analysis

would be expected to cover a wide range of EDL trajectories with which to gather atmospheric characterization data from.

B. Thermal Properties

Heat flow into the ChipSats has a significant effect on their survivability during descent. We propose equipping the ChipSats with a deployable TPS comprising thin flexible shield made of NEXTEL 312 that forms an aerodynamically stable and rigid structure when expanded using SMA struts. To determine what level of thermal protection is necessary we must estimate the heat flux into the ChipSats during descent. Assuming that convective heat transfer predominates, we can calculate the heat flux (q) by:

$$q = kv^3\sqrt{\frac{\rho}{r_n}} \tag{2}$$

where r_n is the entry probe nose radius and $k = 1.8940 \times 10^{-4}$ is a planetary specific constant [20]. We approximate r_n = 8 cm for a ChipSat equipped with the TPS. Consider the heat flux as a function of altitude corresponding to the

same 32805 entry trajectories, as displayed in Fig. 3:

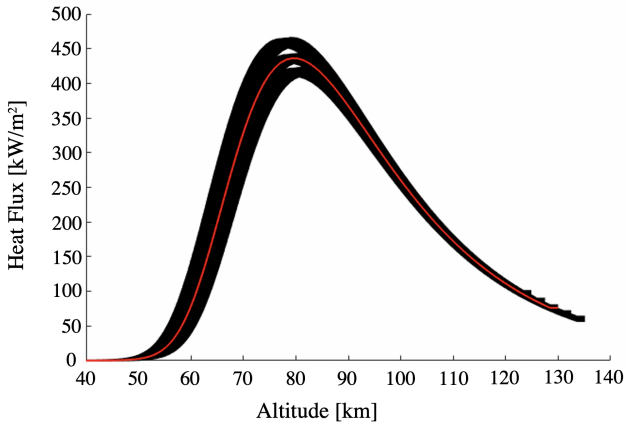

Fig. 3 EDL Sensitivity Analysis Heat Flux Profiles

where the nominal profile is again shown in red and the others in black. This demonstrates a peak heat flux of up to $q = 470$ kW/m^2 at altitudes of 75-80 km. By performing a sensitivity analysis on these trajectories to assess the effect of combined deployment, aerodynamic and atmospheric uncertainties, we can calculate the heat flow into the ChipSats and assess what TPS thickness is required. Figure 4 shows distribution of NEXTEL 312 thickness calculated for the range of trajectories simulated in order to keep the ChipSat PCB below a temperature of 70°C.

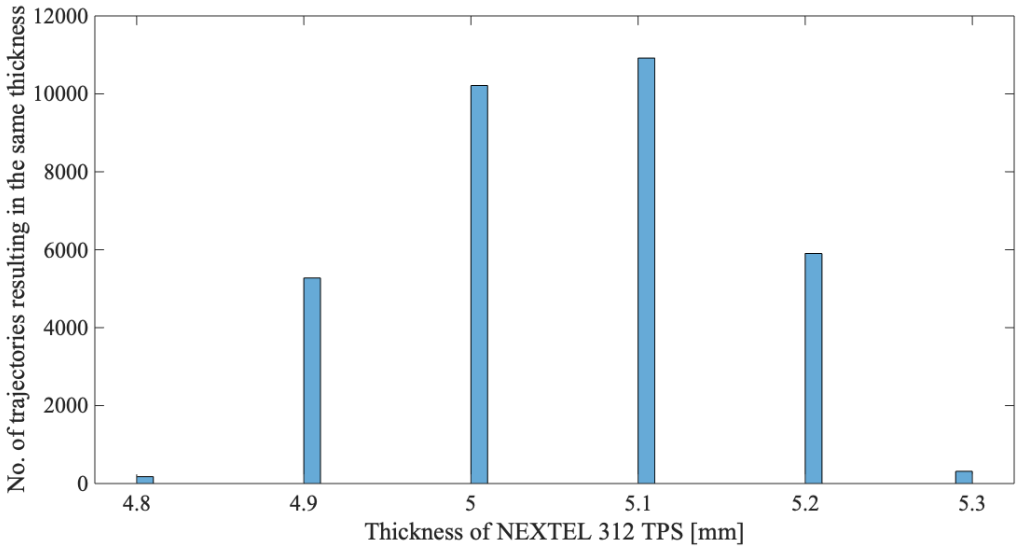

Fig. 4 Sensitivity Analysis Results for TPS thickness

From this analysis, we determined that the ChipSats would survive Mars EDL with a TPS comprising 6 mm thick NEXTEL 312 [21] fabric and an internal PyroGel [22] casing to survive the most extreme thermal loads expected.

C. Atmospheric Characterization

From the trajectory reconstruction data obtained, atmospheric profiles can be derived using the traditional approach of utilizing recorded IMU data, or, if equipped with pressure transducers, those ChipSats will be able to provide data for deriving pressure profiles using a flush air data sensing (FADS) configuration [23] using two pressure probes (see Fig. 8 later) that would deliver in-flight measurements of flow pressure.

Otherwise, density profiles are derived directly from each ChipSat's accelerometer measurements:

$$\rho = -\frac{2ma}{C_d A v^2} \tag{3}$$

where m is the ChipSat mass, $-a$ is its acceleration relative to the atmosphere, A is its cross-sectional area and v is its velocity of the ChipSat relative to the atmosphere (obtained from direct numerical integration). From this, pressure can be found from the derived density profiles by integrating the hydrostatic equilibrium condition:

$$\frac{dp}{dz} = -\rho g \tag{4}$$

where p is the atmospheric pressure and g is the acceleration due to gravity. Local gravity would be assumed using a Mars gravity model [24]. Post-flight reconstruction of ranging data could further improve the accuracy of the local gravity estimate beyond only altitude dependence. Atmospheric temperature can also be found from the ideal gas law:

$$T = \frac{p\mu}{\rho R_0} \tag{5}$$

where T is the atmospheric temperature, μ is the mean molecular weight of the air and R_0 is the universal gas constant.

Derived from the trajectory analysis in the previous section, we can estimate many possible atmospheric profiles that demonstrate the large variability in atmospheric conditions the swarm would experience. Figure 5 provides an example of atmospheric parameter reconstruction that could be expected with the scenario proposed in the modeling section:

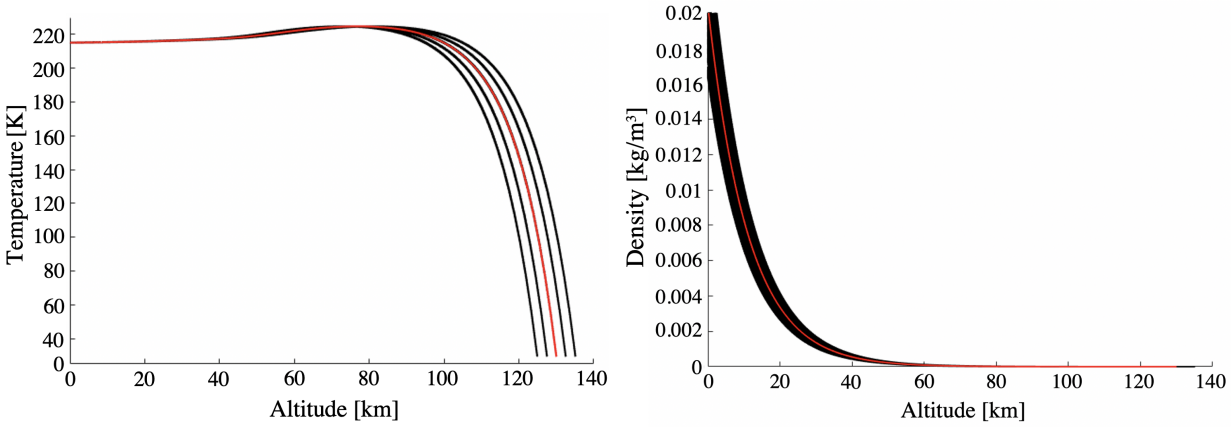

(a) Temperature vs. altitude **(b) Density vs. altitude**

Fig. 5 Atmospheric profiles from sensitivity analysis

D. ChipSat Swarm Relative Positioning

Upon deployment from the CubeSat, the ChipSat swarm will begin to disperse as it translates towards the entry interface with the Martian atmosphere. Until this stage, the IMU cannot measure the acceleration of the ChipSats (due to atmospheric drag). We propose that by networking, the dispersion of the ChipSats could be determined on-board the CubeSat to be able to improve understanding of the initial conditions. This approach is summarized in Fig. 6:

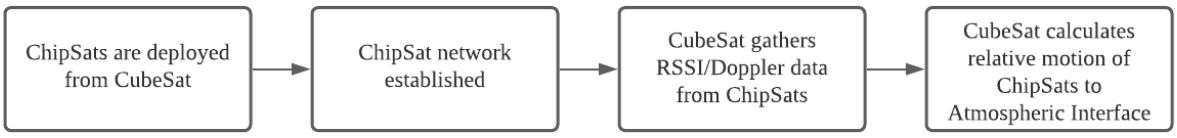

Fig. 6 Relative Navigation Overview

Using the received signal strength indication (RSSI) available on the data packets communicated by each ChipSat, a coarse estimate of ranges between the ChipSats can be derived, and it would be possible to store this data on the CubeSat. When combined with post-processed relative positioning calculations this could quantify the dispersion of the ChipSats from the point of deployment, through to the atmospheric interface and descent. This would be possible by trilaterating the relative positions of ChipSats with respect to one another from the range data available.

IV. ChipSats as a Scientific Platform

A. University of Glasgow ChipSat

The ChipSat platform under development at the University of Glasgow, shown in Fig. 7, comprises a multi-layer 35 × 35 mm PCB, TI CC430 microprocessor with integrated wireless, 3-axis H-bridge-controlled ADCS and a maximum-power-point tracking (MPPT) solar cell power system to enable autonomous operation [25]. For the application discussed in this paper, we envisage replacing the solar panels and the magnetorquers with a large capacity coin cell, a temperature sensor and pressure transducers.

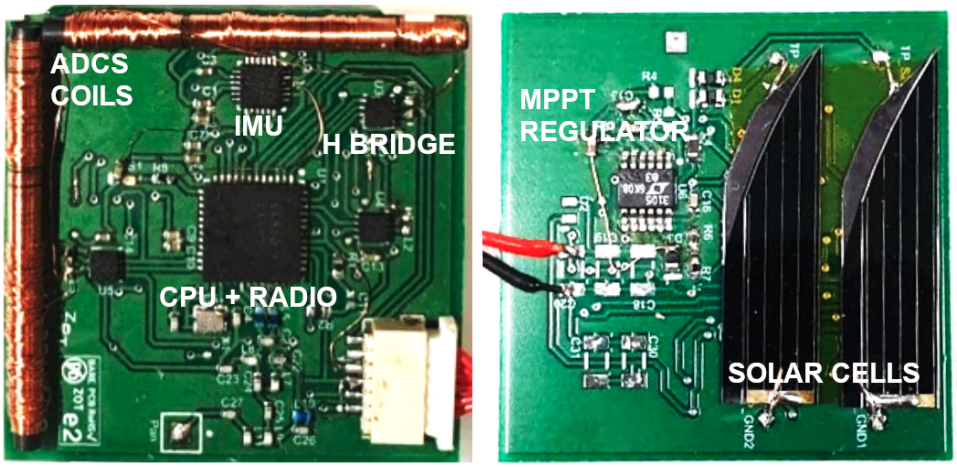

(a) Face 1 **(b) Face 2**

Fig. 7 University of Glasgow ChipSat (3D printed casing and battery holder not shown)

B. ChipSat thermal protection for Mars EDL

Using a flexible TPS comprising a NEXTEL 312 [21] blanket with SMA structural tensioners enables the ChipSats to survive a high peak heat flux during descent and may enable a significant number of ChipSats to survive surface impact while providing compact storage when folded within the CubeSat. This structure also provides passive aerodynamic stability derived from the Viking capsule shape [26]. The flexibility of the NEXTEL blanket is expected to be sufficient for packing the ChipSats within the CubeSat deployer, but will be negligible when deployed with the SMA tensioners.

Renders are presented in Figs. 8a-8d. The deployable lightweight TPS has the extra benefit of further decreasing the ballistic coefficient of the ChipSat. This pointing stability consequently enables a better communication link with a directed antenna always facing space (towards the CubeSat deployer) during entry. The shaping and weighting of this structure can also be tuned to adjust the ballistic coefficient of each ChipSat and generate a wider spread of EDL trajectories. A cross section of the internal configuration is shown in Fig. 8e.

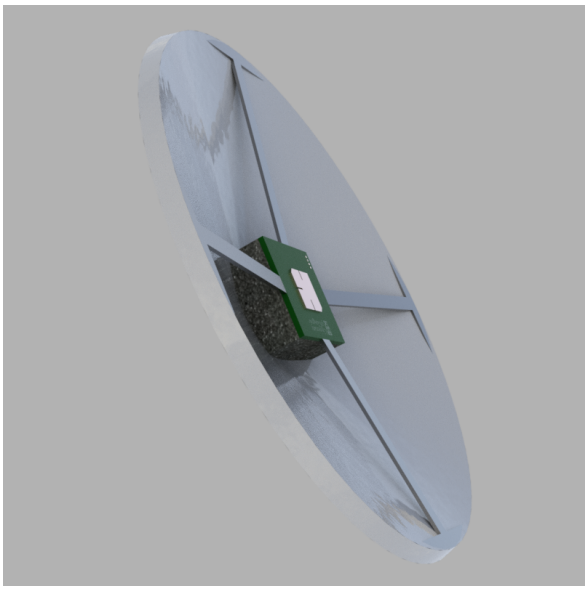

(a) View 1

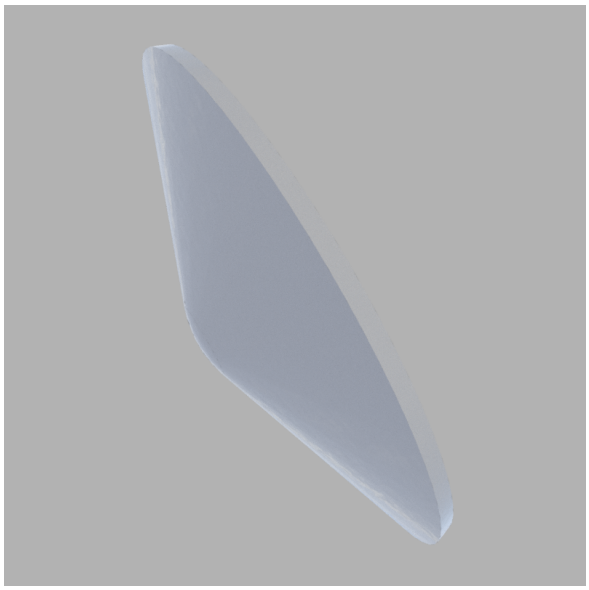

(b) View 2

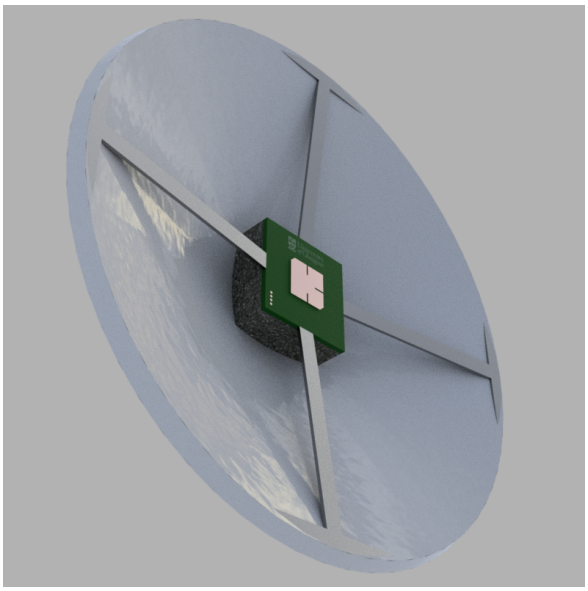

(c) View 3

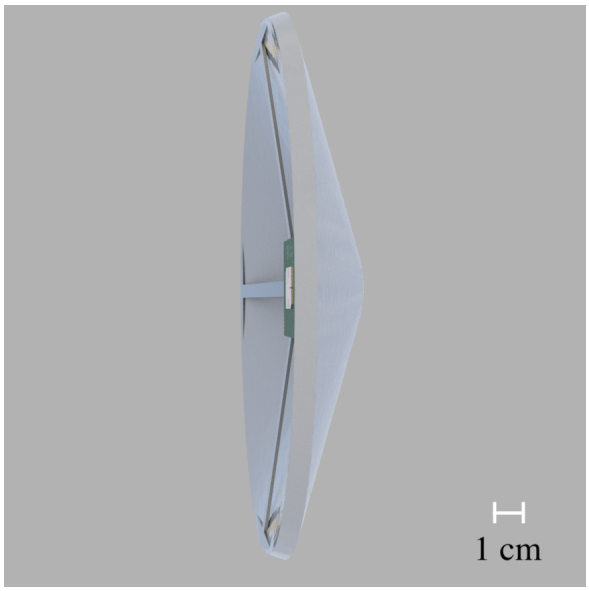

(d) View 4

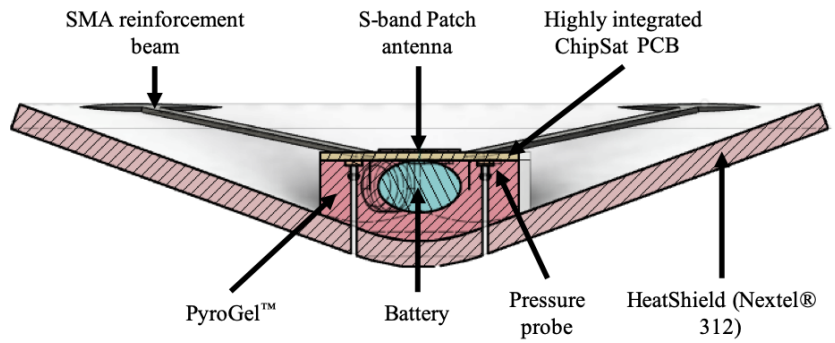

(e) Cross-Sectional Details

Fig. 8 Concept for ChipSat equipped with a flexible thermal protection system

C. Communications Link Budget

Following the model of Mars Cube One, the communications link with Earth will use an antenna on the CubeSat deployer that communicates with NASA's Deep Space Network. In descent the ChipSats would transmit in their wake towards the CubeSat carrier using an S-band patch antenna up to a maximum range of 300 km between the ChipSats and the CubeSat. The link budget for this is shown in Table 2:

Table 2 Link budget

	ChipSat-to-CubeSat	ChipSat-to-ChipSat
Frequency [GHz]	2.4	2.4
Transmitter Power [dBm]	10	10
Transmit Antenna Gain [dBi]	6	-5
Range [km]	300	10
Free Space Path Loss [dB]	-149.6	-120.1
Receive Antenna Gain [dBi]	10	-5
System Noise Temperature [K]	600	600
System Losses [dB]	-3	-3
Data Rate [bps]	1000	1000
$\frac{E_b}{N_0}$	15.9	19.5
$\frac{C}{N}$	12.9	16.5
Link Margin [dB]	4.3	7.9

where $\frac{E_b}{N_0}$ is the ratio of received energy-per-bit to noise density and $\frac{C}{N}$ is the carrier-to-noise ratio. A relatively large link margin of 4.3 dB affords for substantial losses not modeled in this high-level analysis. A 6 dBi patch antenna directed upwards towards a similar antenna on the CubeSat provides an uplink for telemetry including IMU readings, pressure and other data. Potential ChipSat-to-ChipSat communication between surviving probes upon surface impact is achieved via the -5 dBi antenna radiation pattern sidelobes, providing up to 10 km communications range to nearby swarm members with a link margin of 7.9 dB. This is limited by the low transmitter power available and assuming that the ChipSats will tend to land both still pointing outwards towards space and with a clear line of sight to one another over the surface.

The carrier-to-noise ratio is found using:

$$\frac{C}{N} = \frac{E_b}{N_0} + 10\log_{10}\left(\frac{R}{B}\right) \tag{6}$$

where R is data rate in bps and B is receiver noise bandwidth. Using minimum-shift keying (MSK) modulation, $B = 2R$. MSK is chosen for its lower $\frac{E_b}{N_0}req$ than other frequency shift keying modulation techniques supported by the ChipSat's TI CC430 microprocessor. The link margin is then found using:

$$Link\ Margin = \frac{E_b}{N_0} - \frac{E_b}{N_0}req - L_i \tag{7}$$

where $\frac{E_b}{N_0}req$ is the required minimum $\frac{E_b}{N_0}$ for a bit error rate (BER) of 10^{-5}, and L_i is implementation losses. For MSK, accounting for additional errors, $\frac{E_b}{N_0}req$ = 12 dB [27].

Table 3 ChipSat data packet format

Component	Bytes
Preamble	1
Synchronization	1
Temperature + Pressure	3
IMU Acceleration (X,Y,Z)	6
IMU Magnetometer (X,Y,Z)	6

A Time-division multiple access (TDMA) radio communication protocol is used for measurement data transfer from ChipSats to CubeSat. Data is transmitted immediately and not stored due to the risk of ChipSat loss in the hostile environment. Each 8.84 second TDMA frame commences with a time synchronization packet transmitted from the CubeSat. This is used as a time reference for each ChipSat to sequentially transmit a 12 bytes (96 ms) data packet in its appropriate time slot. In addition to preamble, sync, and address (1 byte each), the packet carries pressure and temperature data (3 bytes total from two 12-bit ADCS readings), and 3-axis linear acceleration readings (2 bytes/measurement), as shown in Table 4. A 5 byte (40 ms) delay between packets allows for inter-satellite clock uncertainty, and also permits the CubeSat receiver to adjust receiver frequency to compensate for Doppler shift estimated from ChipSat velocity calculated from received IMU acceleration data. Doppler shift causes a maximum drop of 48 kHz for the ChipSats traveling at 6 km/s. A total of 119 data measurement points can be obtained over the 10 minute EDL phase.

D. Power Budget

The ChipSats are equipped with a small 3.6 V cylindrical battery with a 1.2 Ah capacity, about half the size of a standard AA. For the mission scenario proposed the ChipSats are powered off until launch from the CubeSat via on-board reed switches and an adjacent magnet in the carrier satellite. In active mode, the current draw from the battery would vary between 15-20 mA accounting for various CPU, IMU and communication tasks. Allowing for several more ultra-low power consumption MEMS sensors, a high maximum continuous current draw for each ChipSat can be approximated as 34 mA.

From this we can estimate a discharge time of approximately 35 hours at a continuous 34 mA current draw. As the descent phase would last under an hour, this provides sufficient power supply for EDL and would allow surviving swarm members to continue surface science upon landing. A power budget is shown in Table 4.

Table 4 Power budget

	Operating Power [mW]	Sleep Mode Power [mW]
CPU	47	0.0072
IMU/Temp (1% Duty Cycle)	0.08	-
Transmitter (99% Duty Cycle)	58	-
Receiver (1% Duty Cycle)	18	-
Pressure Sensor (x2, 0.5% DC)	0.1	-
Total [mW]	123.2	0.0072

E. Mass Budget

The ChipSats are comprised of a central PCB, electronics and sensors, a battery, four shape memory alloy struts, a 6 mm thick NEXTEL 312 shield and an internal PyroGel casing. The maximum expected values for mass (MEVs) are shown for the components in Table 5. MEVs are found with a +10% margin on component mass.

Table 5 Mass Budget

Component	MEV [g]
ChipSat	
PCB Core	5
NEXTEL Shield	35
Shape Memory Alloy Supports	10
Battery	10
Pyrogel XTE	2
Total	≤65
CubeSat Carrier	
Structure Chassis	1500
8U Payload (64 ChipSats)	4160
4U Platform (ADCS, CDHS, communications, power)	4000
Total Piggy-back Payload	
Total	≤ 10000

V. Conclusions

An exciting tool for atmospheric characterization has been proposed for a future mission scenario where a swarm of ChipSats is dispersed onto an atmospheric interface trajectory with Mars from a CubeSat carrier, as a candidate piggy-back payload on a future flagship mission to Mars. The scenario proposed highlights the unique ability of a swarm of centimeter-scale femto-spacecraft to deliver utility in ambitious applications well beyond the limited capability of any constituent spacecraft within the swarm. This approach has the considerable advantage of facilitating a low-cost and high-risk design approach that would not be tolerable with a flagship mission, while offering the possibility of high scientific return. This concept could improve understanding of the characteristics of the Martian atmosphere and the

composition of its surface in a way that is not possible with traditional missions such as single probes, by providing simultaneous multi-point sensing.

The results of the sensitivity analysis of EDL trajectories and atmospheric profiles demonstrate the potential that swarm direct entry configurations have to provide atmospheric characterization by supplying multiple data points for analysis. The results also demonstrate that a ChipSat swarm would deliver variability in entry conditions to improve understanding of the Martian atmosphere. The trajectory analysis also enabled the determination of what levels of thermal protection would be required for these devices to survive the thermal loads of atmospheric EDL.

The concept presented here is just one example of what would be possible with a ChipSat swarm in ambitious mission applications. For example, with the same payload mass, over 700 ChipSats without any thermal protection could graze the upper atmosphere of Mars only with no expectation of surviving descent, in exchange for delivering even more multi-point measurements of this region. This concept may also find utility in other interplanetary missions in the future.

Acknowledgments

Colin McInnes acknowledges support from a Royal Academy of Engineering Chair in Emerging Technologies and a Royal Society Wolfson Research Merit Award. Thomas Timmons acknowledges the support of an EPSRC studentship (EP/R513222/1).

References

[1] Schoolcraft, J., Klesh, A. T., and Werne, T., "MarCO: Interplanetary Mission Development On a CubeSat Scale," *SpaceOps 2016 Conference*, AIAA, Daejon, Korea, 2016. https://doi.org/10.2514/6.2016-2491, URL https://arc.aiaa.org/doi/abs/10.2514/6.2016-2491.

[2] Atchison, J., "Microscale Atmospheric Reentry Sensors," *7th International Planetary Probes Workshop*, Barcelona, 2010.

[3] Barker, J., and Rodriguez-Salazar, F., "Self-organizing smart dust sensors for planetary exploration," *Workshop on Nanosensors: Self-Organization and Swarm Robotics, Boston*, 2008.

[4] Manchester, Z., Peck, M., and Filo, A., "KickSat : A Crowd-Funded Mission To Demonstrate The World's Smallest Spacecraft," 2013.

[5] Manchester, Z. R., "Centimeter-scale Spacecraft: Design, Fabrication and Deployment," Ph.D. thesis, Cornell University, 2015.

[6] Hadaegh, F. Y., Chung, S. J., and Manohara, H. M., "On Development of 100-gram-class spacecraft for swarm applications," *IEEE Systems Journal*, Vol. 10, No. 2, 2016, pp. 673–684. https://doi.org/10.1109/JSYST.2014.2327972.

[7] Hein, A. M., Burkhardt, Z., and Eubanks, T. M., "AttoSats: ChipSats, other Gram-Scale Spacecraft, and Beyond," *17th IAA*

Symposium on Visions and Strategies for the Future - 70th International Astronautical Congress, Washington D.C., 2019. URL http://arxiv.org/abs/1910.12559.

[8] Sneeuw, N., and Schaub, H., "Satellite clusters for future gravity field missions," *Gravity, Geoid and Space Missions*, edited by C. Jekeli, L. Bastos, and J. Fernandes, Springer Berlin Heidelberg, Berlin, Heidelberg, 2005, pp. 12–17.

[9] Manchester, Z. R., and Peck, M. A., "Stochastic space exploration with microscale spacecraft," *AIAA Guidance, Navigation, and Control Conference*, Portland, Oregon, 2011. https://doi.org/10.2514/6.2011-6648.

[10] Adams, V. H., and Peck, M., "R-Selected Spacecraft," *AIAA Journal of Spacecraft and Rockets*, Vol. 57, No. 1, 2019. https://doi.org/10.2514/1.A34564.

[11] Weis, L. M., and Peck, M., "Dynamics of chip-scale spacecraft swarms near irregular bodies," *54th AIAA Aerospace Sciences Meeting*, San Diego, California, 2016. https://doi.org/10.2514/6.2016-1468.

[12] Janson, S., and Barnhart, D., "The Next Little Thing : Femtosatellites," *Proceedings of the Small Satellite Conference, Technical Session VI*, 2013.

[13] Ferri, F., Karatekin, Ö., Lewis, S. R., and Forget, F., "ExoMars Atmospheric Mars Entry and Landing Investigations and Analysis (AMELIA)," *Space Sci Rev 215, 8*, 2008. https://doi.org/10.1007/s11214-019-0578-x.

[14] Spiga, A., Banfield, D., Teanby, N. A., Forget, F., Lucas, A., Kenda, B., Manfredi, J. A. R., Widmer-Schnidrig, R., Murdoch, N., and Lemmon, M. T., "Atmospheric Science with InSight," *Space Science Reviews*, Vol. 214 (109), 2018, pp. 1–64. https://doi.org/10.1007/s11214-018-0543-0.

[15] Gentgen, C., Krzymuski, T., Bailet, G., and Laux, C., "TOUTATIS-Ex: a Cubesat Testbed for Entry Experiments on Mars," *Proceedings of the 16th International Planetary Probes Workshop*, Oxford, 2019.

[16] Dutta, S., Braun, R. D., and Karlgaard, C. D., "Uncertainty quantification for mars entry, descent, and landing reconstruction using adaptive filtering," *Journal of Spacecraft and Rockets*, Vol. 51, No. 3, 2014, pp. 967–977. https://doi.org/10.2514/1.A32716.

[17] Bailet, G., "Radiation and ablation studies for in-flight validation," Ph.D. thesis, University of Paris-Saclay, 2019.

[18] Hemmati, H., "Two-Dimensional Planetary Surface Landers Report," *NASA Innovative Advanced Concepts*, 2014.

[19] Williams, D. R., *NASA Mars Fact Sheet*, NASA Goddard Space Flight Center, Greenbelt, MD 20771, 2020. URL https://nssdc.gsfc.nasa.gov/planetary/factsheet/marsfact.html.

[20] Sutton, K., and Graves, R., "A general stagnation-point convective heating equation for arbitrary gas mixtures," NASA TR-R-376, 1971.

[21] *3M^{TM} Nextel^{TM} Ceramic Fabrics 312 and 440*, 3M Advanced Materials Division, 2016. URL https://multimedia.3m.com/mws/media/1242135O/3m-nextel-ceramic-fabrics-312-and-440.pdf.

[22] *Pyrogel XTE High Temperature Insulation*, Aspen Aerogels, 2020. URL https://www.aerogel.com/products-and-solutions/pyrogel-xte/default.aspx.

[23] Whitmore, S. A., Davis, R. J., and Fife, J. M., *In-Flight Demonstration of a Real-Time Flush Airdata Sensing (RT–FADS) System*, NASA Dryden Flight Research Center Edwards, California, 1995. URL https://www.nasa.gov/centers/dryden/pdf/88381main_H-2053.pdf.

[24] Genova, A., Goossens, S., Lemoine, F. G., Mazarico, E., Neumann, G. A., Smith, D. E., and Zuber, M. T., "Seasonal and static gravity field of Mars from MGS, Mars Odyssey and MRO radio science," *Icarus*, Vol. 272, 2016, pp. 228–245. https://doi.org/10.1016/j.icarus.2016.02.050.

[25] Hu, Z., Timmons, T., Stamat, L., and McInnes, C., "Development of a 10g Femto-satellite with Active Attitude Control," *Proceedings of the 17th Reinventing Space Conference*, Belfast, 2019.

[26] Edquist, K. T., Desai, P. N., and Schoenenberger, M., "Aerodynamics for Mars Phoenix entry capsule," *Journal of Spacecraft and Rockets*, Vol. 48, No. 5, 2011, pp. 713–726. https://doi.org/10.2514/1.46219.

[27] Larson, W. J., and Wertz, J. R., *Space Mission Analysis and Design*, 3rd ed., Microcosm Press, California, 1999, Chap. 13.